JOURNAL OF Materials CHEMISTRY

Layered Ni(II)-Zn(II) hydroxyacetates. Anion exchange and thermal decomposition of the hydroxysalts obtained†

Ricardo Rojas,[a] Cristobalina Barriga,[a] Maria Angeles Ulibarri,[a] Pilar Malet[b] and Vicente Rives*[c]

[a]*Departamento de Química Inorgánica e Ingeniería Química, Universidad de Córdoba, Córdoba, Spain*
[b]*Departamento de Química Inorgánica-Instituto de Ciencia de Materiales de Sevilla, Universidad de Sevilla-C.S.I.C., Sevilla, Spain*
[c]*Departamento de Química Inorgánica, Universidad de Salamanca, 37008 Salamanca, Spain. E-mail: vrives@usal.es; Fax: +34 923 29 45 74*

Received 7th November 2001, Accepted 21st January 2002
First published as an Advance Article on the web 21st February 2002

Layered Ni,Zn hydroxyacetates have been prepared by hydrothermal methods and have been used for anion exchange of the original acetate anions by chloride, bromide, carbonate, nitrate, sulfate, and phosphate. Exchange was complete in all cases. The solids have been characterised by elemental chemical analysis, powder X-ray diffraction, thermal analysis (thermogravimetric and differential), FT-IR spectroscopy and electron microscopy; XAS spectra were also recorded in some cases. Thermal decomposition in air leads to removal of interlayer water at 150–200 °C. Mixed NiO–ZnO oxides are formed at higher temperatures. Chloride, sulfate, and phosphate salts are also formed at intermediate calcination temperature, and phosphate remains even after calcination at 1000 °C.

Introduction

Two dimensional solids deserve a lot of attention because of their many and varied applications. One of their most important properties is their ability to exchange species located between the layers; such species can be neutral or ionic, and also the layers can be neutral or electrically charged. Graphite, metal chalcogenides, some oxides (*e.g.*, MoO_3) and even coordination compounds ($Ni(CN)_2$) possess neutral layers. The most widely used group corresponds to systems with negatively charged layers, for example, aluminosilicates, titanates ($K_2Ti_4O_9$), birnessites (A_xMnO_2), and also some hydrogenphosphates. To the third group, formed by positively charged layers, belong the so called hydrotalcites (layered double hydroxides), and some basic salts of copper and zinc.[1–6]

In addition to these families, anion exchangeable layered mixed basic salts were first formed when trying to prepare a nickel basic acetate in the presence of zinc ions under hydrothermal conditions.[7] The structure is related to that of basic zinc salts, such as $Zn_5(OH)_8Cl_2{\cdot}nH_2O$[8] and $Zn_5(OH)_8(NO_3)_2{\cdot}2\ H_2O$.[9] In takovite (a hydrated Ni–Al layered hydroxycarbonate), Ni ions form positively charged brucite-like layers, but in this case (contrary to takovite, where partial Ni/Al substitution exists in the layers) the positive charge of the layers arises from nickel vacancies. Zinc cations occupy tetrahedral sites above and below the nickel vacancies outside the hydroxide layers; acetate ions bound to the zinc ions are exchangeable, and water molecules also exist between the layers. The structure of $Zn_5(OH)_8(NO_3)_2{\cdot}2\ H_2O$ is depicted in Fig. 1. The general formula of these Ni,Zn hydroxyacetates can be written as $Ni_{1-x}Zn_{2x}(OH)_2(CH_3COO)_{2x}{\cdot}n\ H_2O$ and the Zn–Ni ratio is calculated as $2x/(1-x)$.

Preparation of these solids has been described following a hydrothermal method,[7,10,11] or coprecipitation.[10] Their exchange properties with different anions has also been described.[7] However, a study of the solids formed upon thermal decomposition of these salts and of their anion exchanged products is lacking in the literature, despite its potential interest. In the present paper, we report a detailed study of the synthesis and characterisation of Ni,Zn layered hydroxyacetates and of the products obtained upon anion exchange with different anions. The properties of the calcined products are also studied.

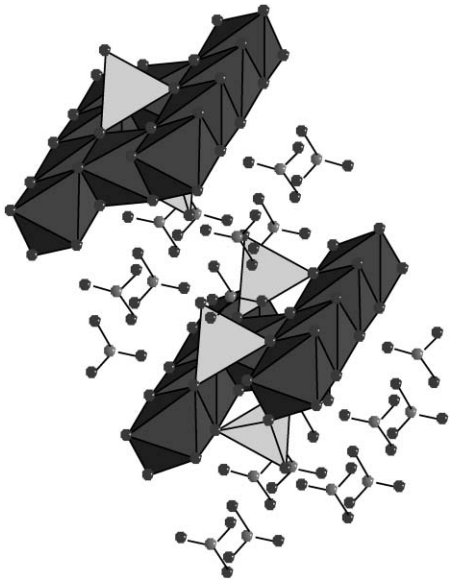

Fig. 1 The structure of $Zn_5(OH)_8(NO_3)_2{\cdot}2\ H_2O$. Interlayer molecular water has been removed. Dark grey: layer octahedra; light grey: outlayer tetrahedra.

†Electronic supplementary information (ESI): PXRD and FTIR of all four NiZn samples; PXRD of calcined chloride, bromide, carbonate and nitrate samples. See http://www.rsc.org/suppdata/jm/b1/b110145e

Experimental

Samples preparation

Acetates. All chemicals used were from Fluka (Switzerland) or Panreac (Spain), of analytical purity, and were used without any further treatment. Gases were from L'Air Liquide (Spain) with a nominal purity of 99.9990%.

The method used to prepare the samples was essentially similar to that described by Yamanaka *et al.*[7] Aqueous solutions of Ni(II) and Zn(II) acetates (1 M) were mixed (total volume 100 ml) in adequate amounts corresponding to Zn–Ni molar ratios ranging from 0.22 to 1.33. Water used to prepare the solutions had previously been boiled to remove dissolved CO_2. The solutions were submitted to hydrothermal treatment in Teflon lined stainless steel bombs at autogenous pressure at 150 °C for 24 h. pH after reaction was lower than in the initial solution due to hydroxy consumption during the precipitation reaction. The solids were separated by centrifugation (Sorvall Super T21 from Dupont) at 10000 rpm. The solid was repeatedly washed with distilled water and dried at room temperature in a vacuum desiccator over silica gel.

Exchanged samples. These were prepared from the samples with a nominal Zn–Ni molar ratio of 0.5 (see below). 300 ml of 1 M solutions of the sodium salts of the anions (chloride, bromide, nitrate, sulfate, carbonate and phosphate) were taken, and the pH adjusted (pH meter Metrohm 691 with automatic dispenser 725 Dosimat from Metrohm) to ensure the presence of the desired anion (especially in the case of CO_3^{2-} and PO_4^{3-}). 1.5 g of the Ni–Zn basic acetate were dispersed at room temperature (41–44 °C in the case of phosphate to avoid Na_3PO_4 precipitation) for 24 h. pH was measured during the exchange reaction, which can be written as:

$$Ni_{1-x}Zn_{2x}(OH)_2(CH_3COO)_{2x}{\cdot}nH_2O + (2x/m)X^{m-} \rightarrow Ni_{1-x}Zn_{2x}(OH)_2X_{2x/m}{\cdot}n'H_2O + 2xCH_3COO^- + (n-n')H_2O$$

The suspension was centrifuged and the solid washed and dried at room temperature in a vacuum desiccator over silica gel.

Calcined samples. The solids were submitted to calcination at selected temperatures (see below) to identify the phases formed. The treatment was carried out in a tubular furnace from CHESA Eurotherm. The heating schedule was as follows: 10 °C min^{-1} up to 50 °C lower than the desired temperature, 10 min isothermal and 2 °C min^{-1} up to the desired temperature, which was maintained for 3 h.

Samples characterisation

Elemental chemical analyses for Ni and Zn were carried out by Atomic absorption spectrometry in a AAS-3100 instrument from Perkin Elmer.

Powder X-ray diffraction (PXRD) patterns were recorded in a Siemens D-5000 instrument, using nickel filtered Cu-Kα radiation (λ = 1.54050 Å).

The FT-IR spectra were recorded by the KBr pellet technique (1% weight sample:KBr) in a Bomem MB-100 Fourier Transform instrument, averaging 64 spectra with a nominal resolution of 4 cm^{-1}, to improve the signal-to-noise ratio.

The VIS–UV spectra were obtained by the diffuse reflectance technique in a Shimadzu UV-240 spectrophotometer with integrating sphere accessory, using MgO as reference, with a slit of 5 nm.

Differential thermal analyses (DTA) and thermogravimetric analyses (TG) were carried out in DTA7 and TGA7 instruments, respectively, from Perkin Elmer, at a heating rate of 10 °C min^{-1}; although the atmosphere around the sample was oxygen, some runs were also carried out in nitrogen to discriminate effects due to combustion processes.

SEM studies were carried out in a JEOL 6300, by deposition of a drop of sample suspension on a Cu sample holder, and covered with a Au layer by sputtering in a Baltec SCD005 apparatus.

X-Ray absorption spectra (XAS) were collected at ESRF station BM29, Grenoble, France. Monochromatization was obtained with double silicon crystals working at the (111) reflection, which were detuned 50% to reduce higher harmonics. Samples were diluted with boron nitride and pressed into self supported wafers. Spectra were recorded at room temperature in transmission mode using optimised ion chambers as detectors. Data were collected up to 16 $Å^{-1}$ with an optimized energy mesh (Δk = 0.026 $Å^{-1}$) in the EXAFS region. Data analysis used the program package XDAP.[12] Backscattering amplitude and phase shift functions for absorber-backscatterer pairs were calculated using the program FEFF6.[13]

Results and discussion

Layered hydroxyacetates

Elemental chemical analysis data for metals and the formula for the compounds are included in Table 1. As can be seen, whatever the Zn–Ni ratio in the starting solution (values ranging from 0.22 to 1.33), the experimental ratio in the solids obtained was in all cases around 0.5, corresponding to a x value of 0.2; this value has been reported[11] to range between 0.15 and 0.25 ($0.35 \leqslant$ Zn–Ni $\leqslant 0.67$), and the values obtained here show a limiting upper value close to Zn–Ni ≈ 0.66 ($x \approx 0.25$). This is the ratio between the tetrahedral and octahedral cations in basic Zn salts, the structures of which are directly related to the double hydroxyacetates synthesized here. Probably, larger x values would lead to collapsing of the structure and/or overcrowding of the interlayer space with charge balancing anions.

The PXRD diagrams of the four compounds prepared are rather similar, see for example that for sample NiZn2 in Fig. 2a. All the PXRD diagrams show a sharp, intense, diffraction maximum close to 13 Å, together with some other extremely weak maxima. Indexing of these diagrams has been made using a least squares method following Yamanaka *et al.*,[7] on the basis of an hexagonal cell similar to that of the basic Zn salts; the lattice parameters a and c have been determined and the values are given in Table 2. The first three maxima, due to diffraction by planes (001), (002), and (003), are rather symmetrical, while the other peaks, due to non-basal planes, are somewhat asymmetric, suggesting some sort of turbostratic disorder in

Table 1 Elemental chemical analysis data (metals) and formula of the hydroxyacetates[a]

Sample	Ni[b]	Zn[b]	Zn–Ni[c]	Zn–Ni[d]	x	Formula[e]
NiZn1	35.99	17.03	0.22	0.43	0.18	$Ni_{0.83}Zn_{0.35}(OH)_2(CH_3COO)_{0.35}{\cdot}1.00H_2O$
NiZn2	34.57	18.77	0.50	0.49	0.20	$Ni_{0.80}Zn_{0.39}(OH)_2(CH_3COO)_{0.39}{\cdot}0.92H_2O$
NiZn3	33.64	20.53	0.86	0.55	0.22	$Ni_{0.79}Zn_{0.43}(OH)_2(CH_3COO)_{0.43}{\cdot}0.96H_2O$
NiZn4	32.54	21.21	1.33	0.59	0.23	$Ni_{0.77}Zn_{0.45}(OH)_2(CH_3COO)_{0.45}{\cdot}0.96H_2O$

[a]Values have been rounded to two figures. [b]Weight percentage. [c]Molar ratio in the starting solution. [d]Molar ratio in the solid. [e]Water content from TG analysis.

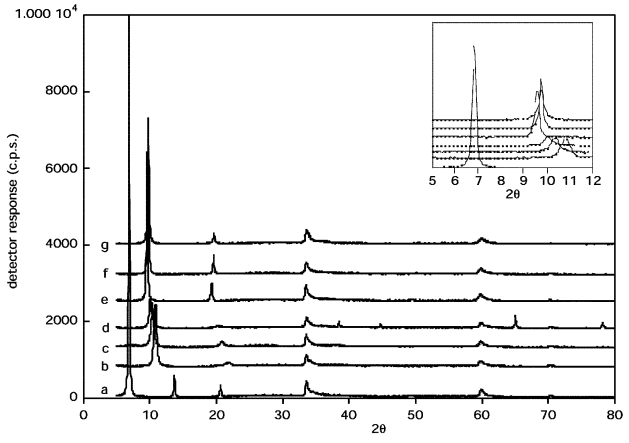

Fig. 2 Powder X-ray diffraction patterns of samples (a) NiZn2; (b) NiZn-Cl; (c) NiZn-Br; (d) NiZn-CO_3; (e) NiZn-NO_3; (f) NiZn-SO_4, and (g) NiZn-PO_4. The inset corresponds to the low angle region.

the interlayer, probably due to the packing of the water molecules and the acetate anions. A small increase in the position of the first maximum is observed when passing from sample NiZn1 (12.6 Å) to sample NiZn4 (13.1 Å). Also, both lattice parameters increase in the same pattern (Table 2); the increase in parameter *a* can be related to an increase in the repulsions within the layers as the charge is increased. As the Zn content increases, the content of acetate ions also increases. In the case of hydrotalcites, it has been observed[14,15] that an increase in the *c* parameter occurs when the concentration of interlayer anions increases, and it has been attributed to a different orientation of the anions in the interlayer because of steric hindrance.

The FT-IR spectra of all four samples are also rather similar and no outstanding difference among them is observed. Again only that for sample NiZn2 is given in Fig. 3a. The broad bands below 900 cm^{-1} are due to lattice vibrations involving the metal cations, and the sharp bands recorded in the middle part of the spectrum are due to the presence of the acetate anions. These bands are slightly shifted from the positions reported in the literature[16] for the free anion, probably because of their coordination to the Zn(II) cation and of the effect of the charged layers, as well as hydrogen bonding with nearby water molecules and/or hydroxy groups. The bands are recorded at 1574 cm^{-1} (antisymmetric stretching of the carboxylate group, recorded at 1556 cm^{-1} in free acetate), 1408 cm^{-1} (symmetric stretching of the acetate group, free acetate at 1413 cm^{-1}), 1344 cm^{-1} (in-plane deformation of methyl group, 1339 cm^{-1} for free acetate), and 1028 cm^{-1} (rocking of methyl group, free acetate at 1020 cm^{-1}). Bands due to modes ν_{asym} and ν_{sym} have been reported for monodentate $Zn(O_2CCH_3)_2(SC(NH_2)_2)_2$ at 1577 and 1420 cm^{-1}, respectively ($\Delta = 157$ cm^{-1}).[17] These data confirm the coordination of the acetate species to the metal cation in a monodentate form; the difference between the positions of the bands ascribed to symmetric and antisymmetric modes of the acetate group (166 cm^{-1}) is consistent with such an ascription, instead of a bidentate, chelating coordination.[10,17]

Table 2 Lattice parameters and stoichiometry factor for the hydroxyacetates

Sample	a^a	c^a	$x^{b,c}$
NiZn1	6.154	12.77	0.185
NiZn2	6.163	12.93	0.199
NiZn3	6.167	13.02	0.213
NiZn4	6.172	13.05	0.215

[a]In Å.
[b]Stoichiometry factor, see text.
[c]Calculated from TG weight losses.

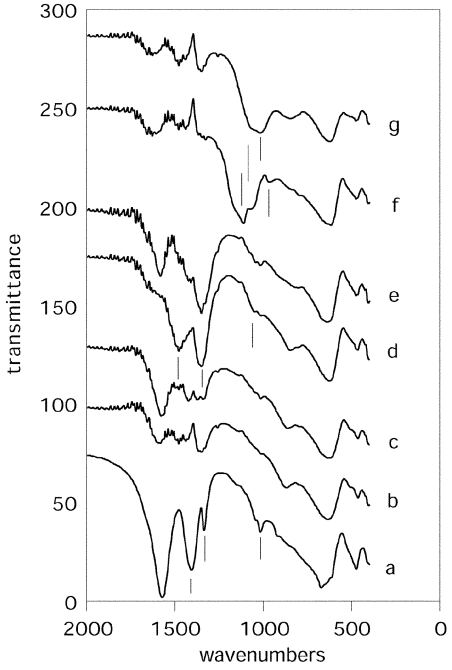

Fig. 3 FT-IR spectra of samples (a) NiZn2; (b) NiZn-Cl; (c) NiZn-Br; (d) NiZn-CO_3; (e) NiZn-NO_3; (f) NiZn-SO_4, and (g) NiZn-PO_4.

Understanding the thermal properties of these solids is very important, in order to be able to ascertain the experimental conditions for their decomposition to lead to mixed oxides. As expected, the DTA and TG/DTG curves are also very similar for the four compounds; representative curves for sample NiZn3 recorded in oxygen are shown in Fig. 4. The DTA curve, recorded in oxygen, shows two rather sharp minima (endothermic effects) at 100 and 207 °C, and this was immediately followed by an exothermic effect around 300 °C with an overlapped extremely sharp maximum at 270 °C. These curves are in some aspects rather similar to those reported elsewhere for thermal decomposition of carbonate-containing hydrotalcites,[18,19] the first minimum is due to removal of interlayer water molecules, and the second one corresponds to water (from dehydroxylation of the layers) and carbon dioxide (from interlayer carbonate) evolution.[20] In the present case, however, observation of the exothermic effect suggests that evolution of acetate takes place with simultaneous oxidation to carbon dioxide and water vapour. When the diagram was recorded in nitrogen (not shown), the exothermic effect around 300 °C was not observed, and the residue after the analysis was brownish, while when recorded in air the residue was bright green. Unfortunately, we could not analyze the evolved gases, so we could not confirm this decomposition process. However, it remains clear, mainly from the temperature range at which these effects are recorded, that the first peak is due to removal

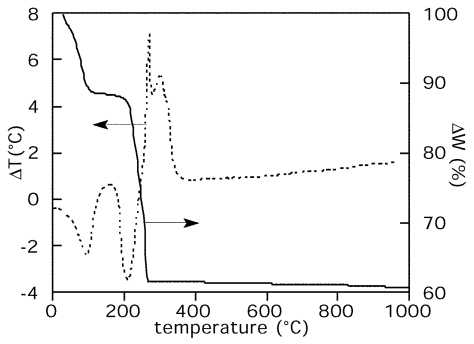

Fig. 4 Thermogravimetric (solid line) and differential thermal (dotted line) analysis of sample NiZn3, recorded in air.

of weakly retained water molecules (*i.e.*, hydrogen bonded in the interlayer space), while the overlapped endothermic–exothermic effects correspond to dehydroxylation of the layers and evolution of CO_2 and H_2O by combustion of the interlayer acetate anions.[21] It is also clear that the hydroxyacetate is fully decomposed at *ca.* 300 °C, as no weight loss is recorded above this temperature; the lack of any defined thermal effect above 300 °C in the DTA curve also rules out any phase change above this temperature.

From the weight losses in both decomposition steps, (i) dehydration, and (ii) dehydroxylation and acetate combustion, it is possible to calculate the amount of interlayer water, and so complete the formula of the samples given in Table 1, and also calculate the Zn–Ni ratio in the samples. Decomposition can be written as:

first weight loss:
dehydration

$$Ni_{1-x}Zn_{2x}(OH)_2(CH_3COO)_{2x}\cdot nH_2O \rightarrow nH_2O + Ni_{1-x}Zn_{2x}(OH)_2(CH_3COO)_{2x}$$

second weight loss:
dehydroxylation

$$Ni_{1-x}Zn_{2x}(OH)_2(CH_3COO)_{2x} \rightarrow Ni_{1-x}Zn_{2x}O(CH_3COO)_{2x} + H_2O$$

acetate combustion

$$Ni_{1-x}Zn_{2x}O(CH_3COO)_{2x} + 4xO_2 \rightarrow Ni_{1-x}Zn_{2x}O_{1+x} + 4xCO_2 + 3xH_2O$$

The values of n (interlayer water content) and x (related to acetate content) can be calculated from the weight losses in both steps. The values obtained for x are summarized in Table 2. The water content is very similar in all four cases, and the x values agree reasonably with those calculated by elemental chemical analysis for Zn and are included in Table 1, thus confirming the 1 : 1 zinc : acetate molar ratio.

According to the literature[7,10,11] the Ni^{2+} ions occupy octahedral holes in the defective hydroxy layer. Further confirmation can be concluded from the VIS–UV spectra recorded in the Diffuse Reflectance mode for these compounds. Two broad bands are recorded, at 390 and 665 nm, although this last band shows an important shoulder at *ca.* 725 nm. For a Ni^{2+} (d^8 configuration) ion in octahedral coordination, these bands should be assigned to transitions $^3A_{2g} \rightarrow {}^3T_{1g}(P)$ and $^3A_{2g} \rightarrow {}^3T_{1g}(F)$, respectively, and from their positions and using the formulae given by Dou,[22] a value of 9070 cm^{-1} is calculated for the crystal field splitting energy, rather close to that reported[21] for nickel double acetate (8172 cm^{-1}) and for β-$Ni(OH)_2$ (8600 cm^{-1}), while the nephelauxetic parameter is calculated to be 0.80, rather close to that reported for β-$Ni(OH)_2$.[23]

A definitive conclusion about the location and coordination of the nickel cations and of zinc (which cannot be detected by VIS–UV spectroscopy because of their d^{10} configuration) has been reached by XAS. A XANES spectrum at the Ni-K edge is similar to those reported[10] for NiZn hydroxyacetates, the Ni^{2+} ions in layers of hydrotalcite-like materials,[24] and also to that reported elsewhere for $[Ni(H_2O)_6]^{2+}$, thus concluding that the Ni(II) cations occupy octahedral sites. On the contrary, the XANES spectrum in the Zn-K edge is very different to that reported for Zn-containing hydrotalcite-like materials,[25] $[Zn(H_2O)_6]^{2+}$ or ZnO; it is again very similar to that reported by Choy,[10] who ascribed it to tetrahedrally coordinated Zn(II) cations.

The best fit to EXAFS spectra leads to data summarised in Table 3. These results are in full agreement with the location of Ni(II) ions in octahedral holes, and of tetrahedrally coordinated Zn(II) ions, within the experimental error usually assumed for coordination numbers (10–15%). The M–O and M–M distances are very similar to those previously[10] reported by Choy *et al.* for Ni,Zn hydroxyacetates, and the Ni–Ni distance is in agreement with lattice parameter a ($2 \times$ d(Ni-Ni)), which is also consistent with edge-sharing octahedra in the layers. From the elemental chemical composition of the sample, the Zn–Ni atomic ratio is 0.49, an average Ni(II) cation is surrounded by 4.5 Ni and 1.5 vacancies within the layer. Assuming that two Zn(II) cations are incorporated for each vacancy, each Ni(II) cation should be closely surrounded by three Zn(II) cations, coinciding with the values experimentally found (the model by Choy *et al.*[10] does not consider these Zn(II) ions around the Ni(II) cations). Using a model based on the structure reported by Yamanaka *et al.*,[7] the Ni–Zn distance calculated corresponds to the location of the Zn(II) cations at both sides of the layer, above and below the Ni(II) vacancies. Under these circumstances, signals due to Zn–Ni and Zn–Zn distances would be expected to contribute to the second shell around Zn(II) cations. However, our model fits the Zn K-edge spectrum using only a Zn–Ni distance at the second coordination shell. The absence of a distinct signal due to the Zn–Zn distances suggests that Zn–Ni and Zn–Zn distances are rather similar, both contributing to the Zn–Ni shell fitted. In order to resolve Zn–Ni and Zn–Zn contributions, the analysis of the Zn K-edge spectrum has been carried out taking the Ni–Ni distance determined at the Ni K-edge (3.08 Å) and defining the angle formed between the Ni-vacant and Ni–Zn axes as the fit parameter. This angle allowed us to calculate geometrically Zn–Ni and Zn–Zn shell radii from the known Ni–Ni distance, the optimum value for a best fit to the experimental data was 29.5°. Consequently, the second shell radii around the Zn(II) cations are calculated as Zn–Ni 3.54 Å and Zn–Zn 3.48 Å, thus confirming the closeness between both shells in a model with the presence of Zn(II) cations at both sides of the vacancy.

Table 3 Summary of EXAFS data for sample NiZn2

	Ni K-edge				Zn K-edge			
Neighbour	N	R/Å	$\Delta\sigma^2$/Å^2	$\Delta E°$/eV	N	R/Å	$\Delta\sigma^2$/Å^2	$\Delta E°$/eV
O	6.0	2.05	0.0052	4.2	4.4	1.95	0.0035	−0.3
Ni	4.9	3.08	0.0058	4.2	6.6	3.54	0.0105	−0.3
Zn	3.2	3.54	0.0111	4.2				

Layered hydroxysalts

As mentioned above, the interlayer acetate ions can be ionically exchanged by other anions.[7] In the following section we describe our results on the nature of the compounds obtained after anionic exchange, introducing different anions, such as chloride, bromide, nitrate, carbonate, sulfate and phosphate. Hence we can analyze the effect of using single- and multiple-valence anions, and mononuclear and multinuclear anions on the exchange ability of these solids. In addition, the nature of the solids obtained after decomposition has been investigated. Sample NiZn2 was used for these anion exchange studies.

Elemental chemical analysis data (metals) for all six exchanged hydroxysalts are given in Table 4, together with the corresponding formula; for these samples, the water content has been calculated from TG analysis (see below), following a similar method to that above for the hydroxyacetates The anion content has not been determined by elemental chemical analysis, but from PXRD and FT-IR results shown below it was concluded that total exchange was achieved. Consequently, the anion content has been calculated on the basis of electroneutrality. The Ni–Zn ratio is very close to the value for

Table 4 Elemental chemical analysis data (metals) and formula of the hydroxysalts[a]

Sample	Ni[b]	Zn[b]	Zn–Ni[c]	x	Formula[d]
NiZn-Cl	35.11	19.01	0.49	0.20	$Ni_{0.81}Zn_{0.39}(OH)_2(Cl)_{0.39}\cdot 0.41H_2O$
NiZn-Br	34.03	20.03	0.54	0.21	$Ni_{0.79}Zn_{0.42}(OH)_2(Br)_{0.42}\cdot 0.61H_2O$
NiZn-NO_3	35.79	21.41	0.54	0.21	$Ni_{0.79}Zn_{0.42}(OH)_2(NO_3)_{0.42}\cdot 0.60H_2O$
NiZn-CO_3	36.62	18.03	0.44	0.18	$Ni_{0.82}Zn_{0.36}(OH)_2(CO_3)_{0.18}\cdot 0.66\ H_2O$
NiZn-SO_4	31.42	16.78	0.48	0.19	$Ni_{0.81}Zn_{0.39}(OH)_2(SO_4)_{0.19}\cdot 0.64H_2O$
NiZn-PO_4	35.92	19.21	0.48	0.19	$Ni_{0.81}Zn_{0.39}(OH)_2(PO_4)_{0.13}\cdot 0.72H_2O$

[a]Values have been rounded to two figures. [b]Weight percentage. [c]Molar ratio in the solid. [d]Water content from TG analysis.

the initial hydroxyacetate, thus suggesting that the exchange reaction is a topotactic process, without large dissolution–reprecipitation from the hydroxyacetate to the hydroxysalt.

The PXRD patterns of the samples are included in Fig. 2. As expected, variations are observed in the basal planes, depending on the precise nature of the interlayer anion. It should also be noted that no peak is recorded around 13 Å, which would be due to the presence of residual hydroxyacetates, thus confirming that 100% exchange was achieved in all six cases. The patterns are very similar to those recorded for the acetate-containing solids, with a very intense peak at low diffraction angles, and extremely weak peaks for higher diffraction angles. While for the hydroxyacetates up to three harmonics (recognized by their rather high symmetry) are recorded, in these cases only two symmetric peaks are recorded from low diffraction angles, peaks at higher diffraction angles showing some asymmetry, probably due to turbostratic disorder of the interlayer species. Ascription of the peaks has been done again on the basis of an hexagonal structure, the first two peaks (from low diffraction angles) are due to planes (001) and (002). The lattice parameters calculated by a least squares method from these PXRD diagrams are given in Table 5; the values for parameter c are in all cases rather close to those reported by Yamanaka *et al.*[7] for Ni,Zn hydroxyacetates exchanged with the same anions.

At a first sight, there seems to be no direct relationship between the value of parameter c and the thermochemical radii of the interlayer anions; these change as:[26]

$$CH_3COO^- < CO_3^{2-} \approx NO_3^- \approx Cl^- < Br^- < SO_4^{2-} \approx PO_4^{3-}$$

while parameter c increases as

$$Cl^- < Br^- < CO_3^{2-} < PO_4^{3-} \approx SO_4^{2-} < NO_3^- << CH_3COO^-$$

Probably, other factors, such as nuclearity of the anion, its ionic charge and its orientation to favour bonding to the Zn^{2+} cations, should also be taken into account. It is not surprising that low c values are obtained for monoatomic anions (chloride and bromide). Carbonate and nitrate possess similar sizes, the larger ionic charge of the former would account for stronger electrostatic layer–anion–layer interactions, and thus a lower c value. For sulfate and phosphate the values of c are almost coincident, which, despite their greater charge, also possess rather large size. However, the most striking result is that for acetate, but, as this anion is markedly nonspherical this limits the usefulness of its thermochemical radius for comparison.

Table 5 Lattice parameters for the hydroxysalts

Sample	a[a]	c[a]	From ref. 7
NiZn-Cl	6.170	8.12	8.12
NiZn-Br	6.172	8.47	8.46
NiZn-NO_3	6.174	9.21	9.29
NiZn-CO_3	6.164	8.93	9.12
NiZn-SO_4	6.168	9.07	9.14
NiZn-PO_4	6.154	9.05	9.25

[a]In Å.

Moreover, orientation of the acetate anion with the oxygen atoms pointing towards the Zn^{2+} cations to complete their tetrahedral coordination means they are orientated perpendicular to the layers, which differs remarkably from the expected spherical, thermochemical radius.

The morphology of the crystallites has been assessed by SEM. Representative micrographs have been included in Fig. 5 for samples containing acetate, carbonate and phosphate. In all cases lamellar crystallites have been formed, with a very large diameter-to-thickness ratio. The average size of the acetate containing crystallites is much larger than that for the exchanged samples. The acetate samples show some sort of curving probably due to an effect of the electron beam on the extremely thin particles.

The FT-IR spectra are shown in Fig. 3. Bands in the middle range (2000–900 cm^{-1}) are characteristic of the interlayer anions. It should be stressed that no band due to acetate species was recorded in any case. Obviously, no anion-related band is recorded for samples NiZn-Cl and NiZn-Br, as the anions are monoatomic entities. The weak absorptions close to

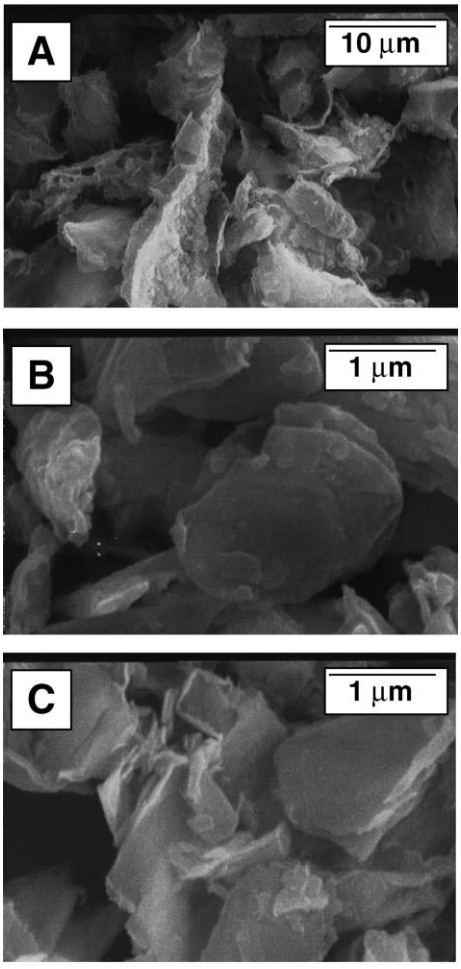

Fig. 5 Scanning electron micrographs of samples NiZn2, NiZn-CO_3 and NiZn-PO_4.

1350–1340 cm^{-1} (also recorded in some of the other spectra) could be due to some carbonate species, probably adsorbed on the external surface of the crystallites and not located between the layers, as it would require larger interlayer spacings (*cf.* Table 5).

The nitrate-containing hydroxysalt exhibits a characteristic absorption at 1354 cm^{-1}, due to mode v_3 of nitrate anions; bands v_2 and v_4 are expected[16] at wavenumbers coinciding with those of the lattice. In the case of the carbonate, however, the v_3 band (carbonate and nitrate possess the same symmetry, D_{3h}, as isolated species) splits into two absorptions at 1497 and 1354 cm^{-1} and this indicates a symmetry lowering upon coordination. This symmetry lowering also gives rise to activation of band v_1, recorded as a very weak shoulder close to 1053 cm^{-1}.

The spectrum for the sulfate-containing sample indicates a distorted tetrahedral symmetry for the interlayer anion (complex absorption around 1000 cm^{-1}). The weak absorption at 961 cm^{-1}, inactive in the free anion, and the band at 1121 cm^{-1} (recorded at 1104 cm^{-1} for the free anion) with two shoulders at 1065 and 1165 cm^{-1}, suggest a decrease in symmetry from T_d to C_{2v}, probably corresponding to the sulfate acting as a bidentate anion.

Finally, the spectrum for sample NiZn-PO_4 shows a single, intense absorption at 1023 cm^{-1}, probably due to mode v_3 of phosphate. It should be recalled that in this case distortion of the symmetry from T_d seems to be less important than in the sample NiZn-SO_4, as only a broad shoulder can be recorded close to 1070 cm^{-1}.

The thermal study has been carried out to assess the temperature range where stable species are formed upon calcination. The TG and DTA curves for all six samples are included in Fig. 6.

In all cases, several steps are recorded. From analogy with the data obtained for the acetate samples discussed above, the first DTA endothermic effect should correspond to the removal of interlayer water molecules, which should be weakly retained by hydrogen bonds. It should be noted, however, that the behaviour of the samples shows some differences, and so, the position of this minimum roughly shifts to slightly higher temperatures as the formal charge of the interlayer anion increases, probably because of the larger electrostatic interaction. Samples NiZn-Cl and NiZn-SO_4 show two additional weight losses, but while in the case of sample NiZn-Cl these take place at *ca.* 250 and 400 °C, in the case of sample NiZn-SO_4 they are recorded at *ca.* 370 and 820 °C.

The diagrams for all other samples show only a DTA minimum (in addition to water removal), although for samples NiZn-Br and NiZn-CO_3 the DTA curves show a shoulder, but so close that a single weight loss is recorded. The diagram for NiZn-NO_3 also shows an exothermic effect in the DTA curve, due to decomposition of the nitrate anions, in a similar way to that described above for the acetate-containing samples.

From data below, these differences can be assigned to the way the interlayer anion is removed during heating. After removal of molecular water, dehydroxylation takes place in the second decomposition step for samples NiZn-SO_4, NiZn-PO_4 and NiZn-Cl, and it overlaps with evolution of the anion in samples NiZn-Br, NiZn-NO_3 and NiZn-CO_3. At higher temperatures, evolution of the anion takes place in samples NiZn-SO_4 and NiZn-Cl.

In all cases, the content of interlayer water has been calculated from the first weight loss, according to the reaction:

$$Ni_{1-x}Zn_{2x}(OH)_2X^{m-}_{2x/m}\cdot nH_2O \rightarrow nH_2O + Ni_{1-x}Zn_{2x}(OH)_2X^{m-}_{2x/m}$$

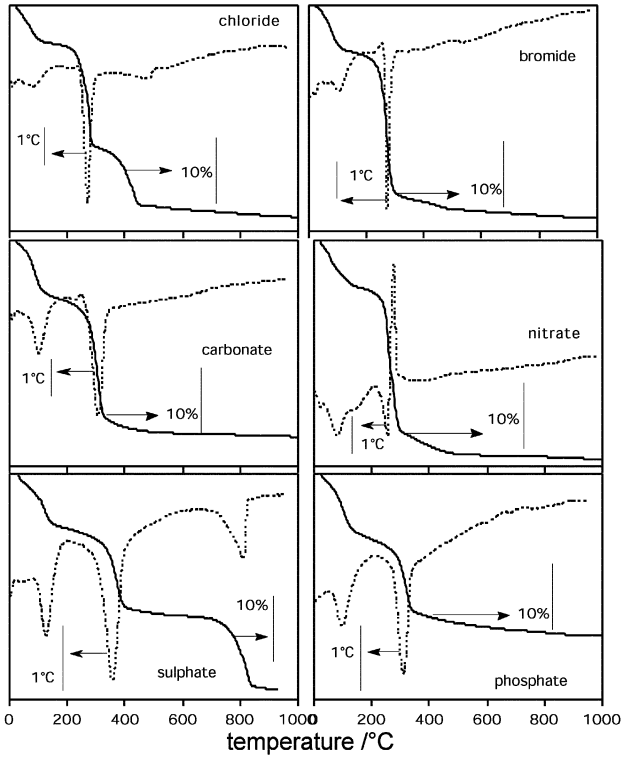

Fig. 6 Thermogravimetric (solid line) and differential thermal (dotted line) analysis of sample NiZn-Cl; NiZn-Br; NiZn-CO_3; NiZn-NO_3; NiZn-SO_4, and NiZn-PO_4 recorded in air.

Calcined samples

In this section we discuss the nature of the crystalline phases formed upon calcination of the hydroxyacetates and of the hydroxysalts at temperatures where the TG curves show a *plateau*, *i.e.*, where thermally stable species are formed. These temperatures differ from one sample to another, according to the stability ranges concluded from the TG curves. However, in all cases a further calcination was conducted at 1000 °C in order to observe formation of well crystallized phases.

The PXRD diagrams for hydroxyacetate NiZn2 calcined at different temperatures are shown in Fig. 7, and those for samples NiZn-SO_4 and NiZn-PO_4 in Fig. 8. The diagram for sample NiZn2 calcined at 150 °C, where dehydration has been completed, shows a shift of the peaks due to diffraction by basal planes to higher angle values, and also a decrease in their intensities; even the peak due to plane (003) is no longer recorded. However, the asymmetric peaks due to non-basal planes, are recorded in the same positions. A similar effect is observed for all other samples. The values of lattice parameters *a* and *c* for the samples calcined after the first thermal effect (150 °C in all cases but for samples NiZn-SO_4 and NiZn-PO_4, which were calcined at 200 °C) are summarized in Table 6, together with the values for the same parameters for the original, uncalcined samples, and the difference between both values.

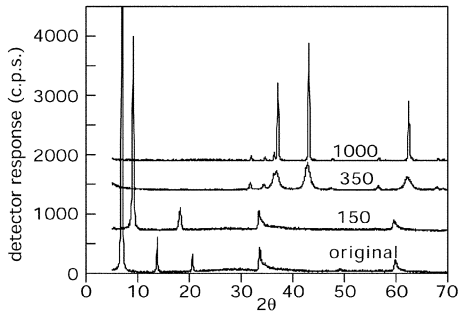

Fig. 7 Powder X-ray diffraction patterns of sample NiZn2 calcined at the temperatures given (in °C), For details, see text.

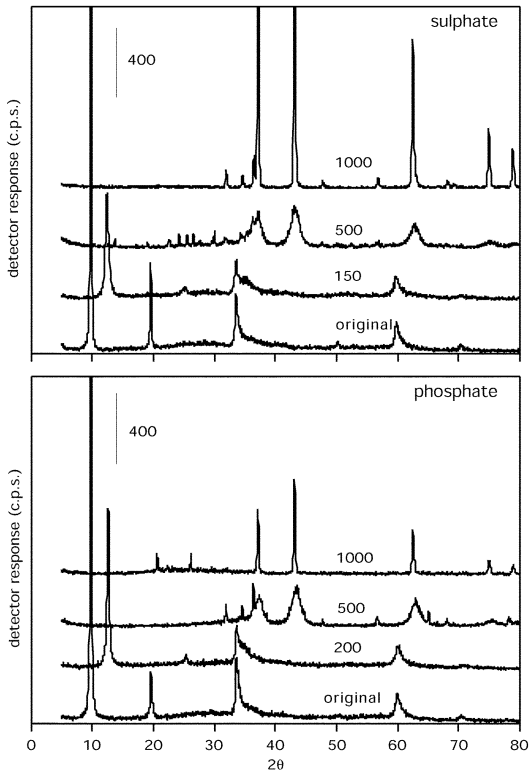

Fig. 8 Powder X-ray diffraction patterns of samples NiZn-SO_4 and NiZn-PO_4 calcined at the temperatures given (in °C), For details, see text.

Values for parameter *a* are coincident, within experimental error, for all samples, both before and after calcination at 150 °C (200 °C for samples NiZn-SO_4 and NiZn-PO_4), again confirming that calcination at this temperature has no important effect on the nature of the layers constituting these materials, and only affects the nature and concentration of the layer cations. However, changes in parameter *c* differ according to the nature of the precise anion existing in the sample. For monoatomic, oxygen-free anions (chloride and bromide) the decrease is very small, especially for sample NiZn-Cl, probably because of the low water content of this sample (Table 4). It is worth noting that the change in the value of *c* is roughly the same for both triangular anions (carbonate and nitrate, 1.67 Å), and for both tetrahedral anions (sulfate and phosphate, 1.97 ± 0.05 Å), while the value is extremely large for acetate (3.08 Å). These differences cannot be solely attributed to removal of water molecules, but are probably related to the particular symmetry of the interlayer anion. It does not seem to be related to the formal charge of the anion, as identical values are measured for nitrate and carbonate, and almost coincident values for sulfate and phosphate.

Calcination at 350 °C leads to drastic changes in the diagrams, Fig. 7. The basal plane peaks have completely disappeared, indicating collapsing and destruction of the layers. Some broad peaks are now recorded, together with weak, sharp peaks. The broad peaks correspond to NiO and ZnO. However, the positions of the peaks are shifted with respect to the values reported in the literature. The main peak of ZnO is reported[27] at 2.4759 Å, but here it is recorded at 2.47 Å (lower spacing), and the main peak of NiO, reported[27] at 2.0880 Å shifts to 2.11 Å (higher spacing). NiO has a cubic, rock salt-type structure, where Ni^{2+} cations occupy octahedral holes, while zincite has an hexagonal structure, with Zn^{2+} cations in tetrahedral holes. Taking into account the values reported[26] for the ionic radii for these cations in octahedral and tetrahedral holes (larger for Zn^{2+} in both cases), the shift in the positions of the maxima can be ascribed to formation of two solid solutions, $Ni_{1-x}Zn_xO$ and $Ni_xZn_{1-x}O$. The behaviour observed for samples NiZn-Br, NiZn-NO_3, and NiZn-CO_3 is somewhat similar to that described for NiZn2.

Table 6 Lattice parameters of original and calcined (after the first thermal effect, 150 or 200 °C, see text) hydroxyacetate (sample NiZn2) and hydroxysalts[a]

	a parameter[b]		*c* parameter[b]		
Sample	Original	Calcined	Original	Calcined	$-\Delta c$[b]
NiZn2	6.16	6.18	12.93	9.85	3.08
NiZn-Cl	6.17	6.16	8.12	7.92	0.20
NiZn-Br	6.17	6.16	8.47	7.78	0.59
NiZn-NO_3	6.17	6.17	9.21	7.54	1.67
NiZn-CO_3	6.16	6.15	8.93	7.26	1.67
NiZn-SO_4	6.17	6.17	9.07	7.15	1.92
NiZn-PO_4	6.15	6.15	9.05	7.03	2.02

[a]Values have been rounded to two figures. [b]in Å.

However, samples NiZn-Cl and NiZn-SO_4 show a different behaviour and in the PXRD diagrams of the solids calcined at intermediate temperatures (just after the second weight loss in the TG diagram, 300 °C for NiZn-Cl, and 500 °C for NiZn-SO_4), additional peaks to those corresponding to the $Ni_{1-x}Zn_xO$ and $Ni_xZn_{1-x}O$ solid solutions are recorded. Ascription of these peaks depends on the precise nature of the interlayer anion. For sample NiZn-SO_4 these peaks can be ascribed to a Zn oxo-sulfate, $Zn_3O(SO_4)_2$, while for the NiZn-Cl sample they are due to $NiCl_2$.

Quite surprisingly, no additional peaks are recorded for sample NiZn-PO_4, the weight loss recorded in the TG diagram up to 500 °C does not correspond to removal of phosphate anions.

Calcination at 1000 °C gives rise to a simplification of the PXRD diagrams. The peaks are now stronger and sharper, indicating an increase in the size of the phases existing in these solids, thus allowing a more precise determination of their positions. Only peaks due to NiO and ZnO (shifted in the same directions as above described for the samples calcined at lower temperatures, *i.e.*, $Ni_{1-x}Zn_xO$ and $Ni_xZn_{1-x}O$ solid solutions still persist at 1000 °C) are recorded. The additional peaks recorded for samples NiZn-Cl and NiZn-SO_4 have vanished, and again only peaks due to NiO and ZnO are recorded. These results are in agreement with the TG analyses above, which indicated new weight losses due to removal of the residual anions. Actually, the weight loss recorded for sample NiZn-SO_4 between 600 and 1000 °C is in agreement with total removal of SO_3 and for NiZn-Cl with total removal of HCl. With sample NiZn-PO_4 (which did not show any weight loss above 500 °C), peaks clearly due to $Zn_3(PO_4)_2$ are now recorded; probably this phase was already present after calcination at 500 °C, but it could be rather amorphous, so being undetectable by PXRD.

Conclusions

Layered Ni,Zn hydroxyacetates with anion exchange ability have been prepared. The Zn–Ni ratio cannot be freely fixed, but a limiting value of 0.66 is reached in all cases. Different inorganic anions (monovalent, polyvalent, monoatomic, polyatomic) have been introduced in the interlayer by anionic exchange of the acetate anions at room temperature, anionic exchange being complete.

Thermal decomposition takes place in several steps: the first one (150–200 °C) corresponds to removal of interlayer water. Condensation of layer hydroxy groups takes place between 250 and 500 °C, forming the mixed oxides, but in samples originally containing chloride, sulfate or phosphate the corresponding salts are also formed. Chloride is removed at 400 °C, sulfate at 800 °C, and phosphate is not removed even at 1000 °C. Well

crystallized mixed NiO–ZnO oxides are formed at 1000 °C in all other cases.

Acknowledgement

Authors thank M.E.C. (grant PB96-1307-C03) and M.C.yT. (grant MAT2000-1148-C02) for financial support. Grants to group FQM-214 and RR from Junta de Andalucía are also acknowledged. We thank ESRF (Grenoble, France) for allocating beam time for XAS measurements (Experiment CH-661).

References

1 A. F. Wells, *Structural Inorganic Chemistry*, 5th, edn., Oxford Sci. Pub., Oxford, 1984.
2 *Pillared Layered Structures: Current Trends and Applications*, ed. I. V. Mitchell, Elsevier Appl. Sci., London, 1990.
3 M. E. Landis, B. A. Aufdembriuk, P. Chu, I. D. Johnson, G. W. Kirsher and M. K. Rubin, *J. Am. Chem. Soc.*, 1991, **113**, 3189.
4 Q. Geng, H. Kanoh, Y. Mijay and K. Ooi, *Chem. Mater.*, 1995, **7**, 1226.
5 S. Carlino, *Chem. Br.*, 1997, 59.
6 *Layered Double Hydroxides: Present and Future*, ed.V. Rives, Nova Sci. Pub. Inc., New York, 2001.
7 S. Yamanaka, K. Ando and M. Ohashi, *Mater. Res. Soc. Symp. Proc.*, 1995, **371**, 131.
8 R. Allmann, *Z. Kristallogr.*, 1968, **126**, 417.
9 W. Stahlin and H. R. Oswald, *Acta Crystallogr. Sect. B: Struct. Crystallogr. Cryst. Chem.*, 1970, **26**, 860.
10 J.-H. Choy, Y.-M. Kwon, K.-S. Han, S.-W. Song and S. H. Chang, *Mater. Lett.*, 1998, **34**, 356.
11 H. Nishizawa and K. Yuasa, *J. Solid State Chem.*, 1998, **141**, 229.
12 A complete description can be found in http://www.xsi.nl.
13 J. J. Rehr, J. Mustre de Leon, S. I. Zabinsky and R. C. Albers, *J. Am. Chem. Soc.*, 1991, **113**, 5135.
14 M. Meyn, K. Beneke and G. Lagaly, *Inorg. Chem.*, 1990, **29**, 5201.
15 H. Kopka, K. Beneke and G. Lagaly, *J. Colloid Interface Sci.*, 1988, **123**, 427.
16 K. Nakamoto, *Infrared and Raman Spectra of Inorganic and Coordination Compounds*, J. Wiley and Sons, New York, 4th edn., 1986.
17 G. B. Deacon and R. J. Phillips, *Coord. Chem. Rev.*, 1980, **33**, 227.
18 L. Pesic, S. Salipurovic, V. Markovic, D. Vucelic, W. Kagunya and W. Jones, *J. Mater. Chem.*, 1992, **2**, 1069.
19 V. Rives, in *Layered Double Hydroxides: Present and Future*, ed.V. Rives, Nova Sci. Pub. Inc., New York, 2001, p. 115.
20 V. Rives, *Inorg. Chem.*, 1999, **138**, 406.
21 L. Poul, N. Jouini and F. Fièvet, *Chem. Mater.*, 2000, **12**, 3123.
22 Y. Dou, *J. Chem. Educ.*, 1990, **67**, 134.
23 N. Minkova, M. Krusteva and G. Nikolov, *J. Mol. Catal.*, 1984, **112**, 23.
24 M. del Arco, V. Rives, R. Trujillano and P. Malet, *J. Mater. Chem.*, 1996, **6**, 1419.
25 M. del Arco, P. Malet, R. Trujillano and V. Rives, *Chem. Mater.*, 1999, **11**, 624.
26 J. E. Huheey, E. A. Keiter and R. L. Keiter, *Inorganic Chemistry, Principles of Structure and Reactivity*, Harper and Row, New York, 4th edn., 1993.
27 Joint Committee on Powder Diffraction Standards, International Centre for Diffraction Data, Pennsylvania, USA, 1977.